Available online at www.sciencedirect.com
SCIENCE DIRECT
Bioorganic & Medicinal Chemistry
Bioorganic & Medicinal Chemistry 14 (2006) 4526–4534

Synthesis and biodistribution of [^{11}C]R107474, a new radiolabeled α_2-adrenoceptor antagonist

M. Van der Mey,[a,*] A. D. Windhorst,[a] R. P. Klok,[a] J. D. M. Herscheid,[a] L. E. Kennis,[b] F. Bischoff,[b] M. Bakker,[b] X. Langlois,[b] L. Heylen,[b] M. Jurzak[b] and J. E. Leysen[a]

[a]*VU University Medical Center, Department of Nuclear Medicine and PET Research, De Boelelaan 1085c, 1081 HV Amsterdam, The Netherlands*

[b]*Johnson and Johnson Pharmaceutical Research and Development, Turnhoutseweg 30, 2340 Beerse, Belgium*

Received 20 May 2005; revised 9 February 2006; accepted 14 February 2006
Available online 6 March 2006

Abstract—R107474, 2-methyl-3-[2-(1,2,3,4-tetrahydrobenzo[4,5]furo[3,2-*c*]pyridin-2-yl)ethyl]-4*H*-pyrido[1,2-*a*]pyrimidin-4-one, was investigated using in vitro and in vivo receptor assays and proved to be a potent and relatively selective α_2-adrenoceptor antagonist. Performed assays in vitro were inhibition of binding to a large number of neurotransmitter receptor sites, drug receptor binding sites, ion channel binding sites, peptide receptor binding sites, and the monoamine transporters in membrane preparations of brain tissue or of cells expressing the cloned human receptors. The compound has subnanomolar affinity for hα_{2A}- and hα_{2C}-adrenoceptors (K_i = 0.13 and 0.15 nM, respectively) and showed nanomolar affinity for the hα_{2B}-adrenoceptors and 5-hydroxytryptamine$_7$ (h5-HT$_7$) receptors (K_i = 1 and 5 nM, respectively). R107474 interacted weakly (K_i values ranging between 81 and 920 nM) with dopamine-hD$_{2L}$, -hD$_3$ and -hD$_4$, h5-HT$_{1D}$-, h5-HT$_{1F}$-, h5-HT$_{2A}$-, h5-HT$_{2C}$-, and h5-HT$_{5A}$ receptors. The compound, tested up to 10 μM, interacted only at micromolar concentrations or not at all with any of the other receptor or transporter binding sites tested in this study. In vivo α_{2A}- and α_{2C}-adrenoceptor occupancy was measured by ex vivo autoradiography 1 h after subcutaneous (sc) administration of R107474. It was found that R107474 occupies the α_{2A}- and α_{2C}-adrenoceptors with an ED$_{50}$ (95% confidence limits) of 0.014 mg/kg sc (0.009–0.019) and 0.026 mg/kg sc (0.022–0.030), respectively. Radiolabeled 2-methyl-3-[2-([1-^{11}C]-1,2,3,4-tetrahydrobenzo[4,5]furo[3,2-*c*]pyridin-2-yl)ethyl]-4*H*-pyrido[1,2-*a*]pyrimidin-4-one ([^{11}C]R107474) was prepared and evaluated as a potential positron emission tomography (PET) ligand for studying central α_2-adrenoceptors. [^{11}C]R107474 was obtained via a Pictet–Spengler reaction with [^{11}C]formaldehyde in 33 ± 4% overall decay-corrected radiochemical yield. The total synthesis time was 55 min and the specific activity was 24–28 GBq/μmol. The biodistribution of [^{11}C]R107474 in rats revealed that the uptake of [^{11}C]R107474 after in vivo intravenous administration is very rapid; in most tissues (including the brain) it reaches maximum concentration at 5 min after tracer injection. In agreement with the known distribution of α_2-adrenoceptors in the brain, highest uptake of radioactivity was observed in septum (3.54 ± 0.52 ID/g, 5 min pi) and entorhinal cortex (1.57 ± 0.10 ID/g, 5 min pi). Tissue/cerebellum concentration ratios for septum (5.38 ± 0.45, 30 min pi) and entorhinal cortex (3.43 ± 0.24, 30 min pi) increased with time due to rapid uptake followed by a slow washout. In vivo blocking experiments using the non-selective α_2-adrenoceptor antagonist mirtazapine demonstrated specific inhibition of [^{11}C]R107474 binding in selective brain areas. The receptor binding profile of mirtazapine is reported and the selectivity of inhibition of binding is discussed. These results suggest that [^{11}C]R107474 deserves further investigation as a potential radioligand for studying α_2-adrenoceptors using PET.

1. Introduction

The role of the monoamines serotonin and noradrenaline in mental illnesses including depression is well recognized. All antidepressant drugs in clinical use increase acutely the availability of one or both of these monoamines at the synapse either by inhibiting their neuronal reuptake, inhibiting their metabolism, or increasing their release by blocking the α_2-auto- and heteroadrenoceptors on the monoaminergic neuron.[1] Chronic antidepressant treatment gradually downregulates α_2-adrenoceptor autoreceptors.[2] This adaptive effect is related to their delay to onset of action and underpins the utility of antagonistic properties at α_2-adrenoceptor sites for hastening therapeutic properties.[3,4] As regards autoreceptors, the α_{2A}-adrenoceptor

Keywords: [^{11}C]R107474; [^{11}C]Formaldehyde; α_2-Adrenoceptor antagonist; PET.
* Corresponding author. Tel.: +31 0 20 444 9720; fax: +31 0 20 444 9121; e-mail: mmeij@rnc.vu.nl

0968-0896/$ - see front matter © 2006 Elsevier Ltd. All rights reserved.
doi:10.1016/j.bmc.2006.02.029

subtype predominates over α_{2C}-adrenoceptors and its levels are elevated both in depressed patients and by long-term stress.[5,6]

PET offers the potential to image drug–receptor interactions in vivo in man but the methodology remains limited by the number of site selective radioligands available. A successful PET marker could help clarify any putative changes in receptor density and can be applied to assess occupancy of central α_2-adrenoceptors by antidepressant drugs which have affinity for this receptor. Development of suitable imaging ligands to facilitate in vivo characterization of α_2-adrenoceptors has been limited in its success. Although a number of different α_2-adrenoceptor antagonists have been evaluated as potential PET ligands, none has progressed to routine use in humans. Of the α_2-adrenoceptor antagonists which have been evaluated as in vivo CNS ligands, [^{11}C]MK-912 (rodents and monkey),[7] [^{11}C]WY-26703 (rat and monkey),[8] [^{18}F]fluoroatipamezole (rat),[9] [*N*-methyl-^{11}C]mianserin (swine),[10] [^{3}H]RX 821002 (rat),[11] and [*O*-methyl-^{11}C]RS-15385-197 (rat and human)[12,13] showed little potential for further development. Additional studies are needed to establish the usefulness of fluorine-18 labeled RS-15385-FP[14] and [*N*-methyl-^{11}C]mirtazapine[15] for PET neuroimaging in human.

2-Methyl-3-[2-(1,2,3,4-tetrahydrobenzo[4,5]furo[3,2-*c*]pyridin-2-yl)ethyl]-4*H*-pyrido[1,2-*a*]pyrimidin-4-one[16] (R107474, Fig. 1) was under clinical evaluation for the treatment of depression, characterized by anergia and lack of drive. However, further clinical development has been stopped. Since the compound has a high affinity and selectivity for the α_2-adrenoceptor versus the α_1-adrenoceptor, binds reversible, and shows potent central in vivo activity, radiolabeled R107474 might be a suitable PET ligand for human use.

In this paper, we report the in vitro and ex vivo receptor binding properties of R107474. The receptor binding profile of R107474 was investigated comprising 25 monoamine neurotransmitter receptors, three glutamate receptors, three opiate receptors, seven peptide receptors, the sigma1 site, two ion channel binding sites, and three monoamine transporters. The compound was investigated for in vitro binding using membrane preparations of animal tissue (r, rat; m, mouse; p, pig; and gp, guinea-pig) or in most instances using membranes of cell lines transfected with cloned human (h) receptors. In vivo α_{2A}- and α_{2C}-adrenoceptor occupancy in rat was measured by ex vivo autoradiography 1 h after sc administration of R107474. Also the receptor binding of mirtazapine, a clinically used antidepressant with α_2-adrenergic blocking properties,[17,18] was investigated in the same models. We describe the optimization of the radiosynthesis of 2-methyl-3-[2-([1-^{11}C]-1,2,3,4-tetrahydrobenzo[4,5]furo[3,2-*c*]pyridin-2-yl)-ethyl]-4*H*-pyrido[1,2-*a*]pyrimidin-4-one[19] ([^{11}C]R107474) and have investigated its biodistribution, specific uptake in brain areas, and inhibition of binding in the brain with mirtazapine. Selectivity of uptake in specific brain areas and specificity of inhibition of binding by mirtazapine in relation to α_2-adrenoceptor labeling are discussed.

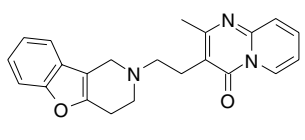

R107474

Figure 1. Molecular structure of R107474.

2. Results and discussion

2.1. In vitro receptor binding profile of R107474 and mirtazapine

The binding affinities in vitro (pIC_{50} values in $-\log M$ and K_i values in nanomolars) of R107474 for the various receptors, ion channel, and monoamine transporter binding sites determined according to published methods[20] are shown in Table 1. R107474 showed high affinity for hα_{2A}-, hα_{2B}-, and hα_{2C}-adrenoceptors, stably expressed in CHO cells. The compound bound preferentially to the hα_{2A}- and hα_{2C}-adrenoceptor subtypes (K_i = 0.13 and 0.15 nM, respectively) and was seven times less potent in binding to the hα_{2B}-adrenoceptors (K_i = 1.03 nM). R107474 bound to h5-HT$_7$ receptors with nanomolar affinity (K_i = 5 nM). Further, R107474 showed moderate to low binding affinity for h5-HT$_{1D}$ (K_i = 48 nM), h5-HT$_{2C}$ (K_i = 97 nM), and hD$_{2L}$ receptors (K_i = 81 nM). The compound interacted weakly (K_i values ranging between 0.15 and 5 μM) with hα_{1A}, hD$_3$, hD$_4$, h5-HT$_{1A}$, h5-HT$_{1B}$, h5-HT$_{1E}$, h5-HT$_{1F}$, h5-HT$_{2A}$, h5-HT$_{4L}$, h5-HT$_{5A}$, h5-HT$_6$, rNa$^+$-ion channel binding sites, and 5-HT transporter sites. Up to a concentration of 10 μM, R107474 did not bind to any of the other receptor sites, ion channels or transporter binding site investigated in this study.

Mirtazapine is on the market as an antidepressant agent with mixed antagonism at certain serotonergic and adrenergic receptors. The receptor profile (Table 1) shows that it primarily binds to histamine H$_1$ receptors with nanomolar affinity (K_i = 1.6 nM). It binds with moderate affinity (K_i between 20 and 300 nM) to 5-HT$_{2A}$, 5-HT$_{2C}$, α_{2A}-A, α_{2B}-A, α_{2C}-A, 5-HT$_3$, and 5-HT$_7$ receptors. Findings are in agreement with published data.[21] Although mirtazapine's affinity for α_2-adrenergic receptors is 85–150 times lower than that of R107474, the compound was chosen as a displacing agent, because it is the only compound used in the clinic that is dosed for its α_2-adrenergic receptor antagonistic effect.[17,18] At the dose of 20 mg/kg administered in this study, which is more than 10,000 times higher than the tracer dose, displacement can be expected.

2.2. Ex vivo α_2-adrenoceptor occupancy of R107474

In vivo α_{2A}- and α_{2C}-adrenoceptor occupancy was measured by ex vivo autoradiography 1 h after sc administration of R107474. Selective occupancy measurement of α_{2A}-adrenoceptors was achieved by quantifying the

Table 1. In vitro binding affinities (pIC_{50} values ± SD and K_i values in nanomolars) of R107474 compared to mirtazapine for various receptors, ion channel- and monoamine transporter binding sites[a]

Receptor	Species	Tissue or cell	R107474				Mirtazapine K_i
			pIC_{50}	SD	K_i	n	
Neurotransmitter receptor sites							
Adrenergic-α_{1A}	Human	CHO	6.45[b]	0.25	182	3	1815
Adrenergic-α_{2A}	Human	CHO	9.26[b]	0.13	0.13	5	20
Adrenergic-α_{2B}	Human	CHO	8.57[b]	0.11	1.03	5	88
Adrenergic-α_{2C}	Human	CHO	8.77[b]	0.06	0.15	5	18
Adrenergic-β_1	Human	CHO	<5			3	>10,000
Adrenergic-β_2	Human	CHO	<5			3	>10,000
Adrenergic-β_3	Human	CHO	<5			3	>10,000
Dopamine-D_1	Rat	Striatum	<5			4	4167
Dopamine-D_{2L}	Human	CHO	6.58	0.13	81	4	>10,000
Dopamine-D_3	Human	CHO	6.50	0.17	228	3	5723
Dopamine-D_4	Human	CHO	6.34	0.08	158	3	2518
5-HT_{1A}	Human	L929 sA	5.72	0.29	1478	3	3334
5-HT_{1B}	Human	HEK293	5.61	0.13	1286	3	3534
5-HT_{1D}	Human	C6 glioma	6.96	0.40	48	5	955
5-HT_{1E}	Human	L929 sA	5.04	0.02	3330	3	728
5-HT_{1F}	Human	HEK293	5.53	0.14	1678	4	583
5-HT_{2A}	Human	L929 sA	5.98	0.45	434	3	70
5-HT_{2C}	Human	Sf9	6.79	0.16	97	3	40
5-HT_3	Mouse	NxG 108CC15	<5			4	170
5-HT_{4L}	Human	HEK293	5.70	0.12	1003	4	>10,000
5-HT_{5A}	Human	HEK293	6.16	0.48	352	3	670
5-HT_6	Human	HEK293	5.16	0.05	3056	2	
5-HT_7	Human	CHO	7.89	0.14	5.0	4	265
Histamine-H_1	Human	CHO	<5			4	1.6
Cholinergic muscarinic	Rat	Striatum	<5			4	1100
Ion channel ligand binding sites							
Ca^{2+}-ligand binding sites	Rat	Cortex	<5			4	>10,000
Na^+-channel	Rat	Cortex	5.29	0.13	5118	4	6905
Monoamine transporters							
DA-transporter	Rat	Striatum	<5			4	>10,000
5-HT-transporter	Human	Platelets	5.21	0.12	1412	3	>10,000
NE-transporter	Rat	Cortex	<5			4	1640

[a] The compounds did not bind to a concentration of 10 μM to opiate receptors (hμ-opiate, gpκ-opiate, and hδ-opiate), glutamate receptors (MK801- and glycine site of the rNMDA receptor and rAMPA receptors), and peptide receptors (hBK_2, $rCCK_A$, $hCCK_B$, hNK_1, hNK_2, hNK_3, and hVIP) and $h\sigma_1$ binding sites.

[b] See Ref. 16.

specific binding of the subtype non-selective radioligand [^{3}H]RS79948-197 in the septum, a brain area expressing selectively the α_{2A}-adrenoceptor. To measure the occupancy of α_{2C}-adrenoceptors, we have used the property of [^{3}H]rauwolscine to label selectively this subtype in the rodent brain. α_{2C}-Adrenoceptor occupancy was quantified in the striatum, the brain area showing the highest α_{2C}-adrenoceptor density.[22] It was found that R107474 occupies the α_{2A}-adrenoceptor and α_{2C}-adrenoceptor with an ED_{50} (95% confidence limits) of 0.014 mg/kg sc (0.009–0.019) and 0.026 mg/kg sc (0.022–0.030), respectively (see Fig. 2).

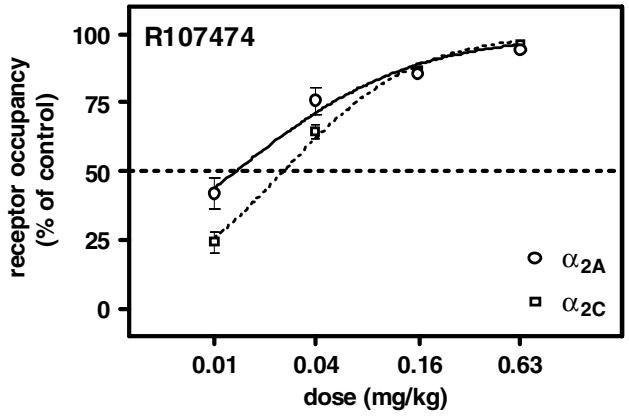

Figure 2. In vivo α_{2A}- and α_{2C}-adrenoceptor occupancy measured by ex vivo autoradiography using [^{3}H]RS79948-197 and [^{3}H]rauwolscine, respectively, 1 h after sc administration of R107474.

2.3. Signal transduction on cloned human receptors in cell lines

Cyclic AMP is the major second messenger known to be inhibited by α_2-adrenoceptors. R107474 has been shown to reverse the clonidine-induced inhibition of cyclic AMP production mediated by human α_{2A}- and α_{2C}-adrenoceptors expressed in cell lines (K_b is 2.8 and 4.4 nM, respectively) and was a full antagonist on both receptor subtypes (unpublished results). In [^{35}S]GTPγS assays, R107474 has been shown to be a full antagonist of all three α_2-subtypes, with a K_b of 2.38, 9.54, and 1.97 nM for the $h\alpha_{2A}$-, $h\alpha_{2B}$-, and $h\alpha_{2C}$-adrenoceptors, respectively.

2.4. Radiosynthesis

[^{11}C]R107474 was synthesized by the Pictet–Spengler condensation reaction,[23] which is an excellent method to introduce carbon-11 into a tetrahydroisoquinoline.[19] The reaction scheme for [^{11}C]R107474 is shown in Figure 3. [^{11}C]Formaldehyde was reacted with 3-{2-[(2-benzo[*b*]furan-2-ylethyl)amino]ethyl}-2-methyl-4*H*-pyrido[1,2-*a*]pyrimidin-4-one (**1**, obtained via unpublished synthesis route) providing [^{11}C]R107474.

2.4.1. [^{11}C]Formaldehyde. Nader et al.[24] have proposed a new procedure for the reduction of [^{11}C]carbon dioxide to [^{11}C]formaldehyde with LAH in diethyl ether at −48 °C, thus stopping the stepwise reduction (formate–formaldehyde–methanol) at the formaldehyde stage. The highest radiochemical yield of [^{11}C]formaldehyde was 58% after quenching the reaction with aqueous sulfuric acid and distillation to a second reaction vessel containing 1 mL of water. At temperatures between −52 and −47 °C, the radiochemical purity consistently exceeded 95%. Significant quantities of [^{11}C]methanol were found above −45 °C. At temperatures higher than −33 °C, [^{11}C]methanol was the only product. In contrast, Roeda and Crouzel[25] found that reduction of [^{11}C]carbon dioxide with LAH in diethyl ether or THF at low temperatures, and to a lesser extent at room temperature, leads to considerable amounts of [^{11}C]formic acid. Further reduction takes place at higher temperatures but seems to favor the formation of [^{11}C]methanol rather than that of [^{11}C]formaldehyde. The best [^{11}C]formaldehyde yield was of the order of 20% at −10 °C after distillation. [^{11}C]Formaldehyde was never obtained as the major product.

The [^{11}C]formaldehyde yields that we achieved by reduction of [^{11}C]CO_2 with LAH in THF at low temperatures are summarized in Table 2. At a temperature of −40 °C and quenching the excess LAH with aqueous sulfuric acid, [^{11}C]formaldehyde was obtained in 21 ± 4% decay-corrected yield after distillation. Lower (T = −50, −60 °C) as well as higher (T = −20, −30 °C) reaction temperatures did not improve the [^{11}C]formaldehyde yield. [^{11}C]Methanol was found to be the major side product. Quenching the reaction with a hydrogen chloride solution in 1,4-dioxane led to a significant improvement of the radiochemical yield (41 ± 4% at −40 °C;[19] see Table 2). This is probably due to more efficient quenching since the HCl in 1,4-dioxane and the LAH in THF solution in the vial mix much better than the aqueous sulfuric acid solution with the content of the vial at low temperatures. The temperature optimum for the reduction of [^{11}C]CO_2 to [^{11}C]formaldehyde and quenching with HCl in 1,4-dioxane was found at −70 °C providing [^{11}C]formaldehyde in 61 ± 7% decay-corrected yield (see Table 2).

Table 2. Influence of reaction temperature and quenching agent on the [^{11}C]formaldehyde yield

Entry	T (°C)	Quenching agent[a]	[^{11}C]CH_2O[b] (%)
1	−20	H_2SO_4	9 ± 3
2	−30	H_2SO_4	15 ± 3
3	−40	H_2SO_4	21 ± 4
4	−50	H_2SO_4	17 ± 3
5	−60	H_2SO_4	7 ± 4
6	−40	HCl	41 ± 4[c]
7	−50	HCl	48 ± 5[c]
8	−60	HCl	55 ± 5[c]
9	−70	HCl	61 ± 7[c]
10	−80	HCl	50 ± 6

[a] H_2SO_4 in water (300 μL, 2 M) and HCl in 1,4-dioxane (150 μL, 4 M), $n \geqslant 4$.
[b] Overall decay-corrected yield. [^{11}C]CO_2 was reduced with LAH (50 μL, 1 M) in dry THF (250 μL).
[c] See Ref. 19.

2.4.2. [^{11}C]R107474. The influence of reaction temperatures and quench solvents on the radiochemical yield and specific activity of [^{11}C]R107474 is shown in Table 3. Using the optimum temperature of −70 °C for the preparation of [^{11}C]formaldehyde whilst quenching with HCl in 1,4-dioxane (Table 2, entry 9), it was found that the Pictet–Spengler condensation reaction gave the highest radiochemical yield at 140 °C as described previously[19] (Table 3, compare entries 1–6). Under these circumstances, [^{11}C]R107474 was obtained in 50% overall decay-corrected radiochemical yield with a specific activity of 3–4 GBq/μmol at the end of synthesis (55 min after end of bombardment, EOB). Obviously, despite the good radiochemical yield, the reaction conditions were not favorable with respect to the specific activity. Since the 1,4-dioxane was most probably the main source of carrier formaldehyde, the hydrogen chloride solution in 1,4-dioxane was replaced by a hydrogen chloride solution in diethyl ether (Table 3, entries 7–10). Now, [^{11}C]formaldehyde formation at −70 °C and

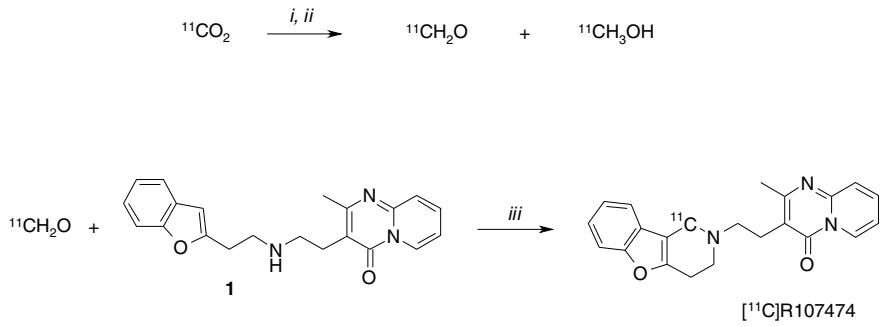

Figure 3. Radiosynthesis of [^{11}C]R107474. Reagents and conditions: (i) LAH, THF, −20 °C; (ii) HCl, diethyl ether; (iii) HCO_2H, H_2O, 140 °C.

Table 3. Effect of reaction temperatures and quench solution on radiochemical [^{11}C]R107474 yield and specific activity

Entry	[^{11}C]CH_2O T (°C)	Quench solvent[a]	Pictet–Spengler T (°C)	[^{11}C]R107474[b] (%)	Specific activity (GBq/μmol)
1	−70	1,4-Dioxane	100	9 ± 2	ND
2	−70	1,4-Dioxane	110	29 ± 2	ND
3	−70	1,4-Dioxane	120	33 ± 4	ND
4	−70	1,4-Dioxane	130	45 ± 3	ND
5	−70	1,4-Dioxane	140	50 ± 4	3–4
6	−70	1,4-Dioxane	150	46 ± 4	ND
7	−70	Diethyl ether	140	10 ± 3	ND
8	−30	Diethyl ether	140	19 ± 3	14–18
9	−20	Diethyl ether	140	33 ± 4	24–28
10	−10	Diethyl ether	140	19 ± 2	20–27

[a] Excess LAH was quenched with HCl in 1,4-dioxane (90 μL, 4 M) or HCl in ether (180 μL, 2 M).
[b] Overall decay-corrected yield. [^{11}C]CO_2 was reduced with LAH (300 μL, 0.1 M), $n \geqslant 4$.

Pictet–Spengler condensation at 140 °C provided [^{11}C]R107474 in an overall decay-corrected radiochemical yield of only 10 ± 3% (entry 7). Using HCl in diethyl ether instead of 1,4-dioxane, the optimum [^{11}C]formaldehyde formation/quenching temperature was found to be −20 °C (Table 3, compare entries 7–10). This could be caused by incomplete quenching as HCl in diethyl ether might be less reactive than HCl in 1,4-dioxane at −70 °C. Under the conditions mentioned in entry 9, [^{11}C]R107474 was obtained in 33 ± 4% overall decay-corrected radiochemical yield with a specific activity of 24–28 GBq/μmol at the end of synthesis (55 min after EOB). Thus, quenching with HCl in diethyl ether instead of 1,4-dioxane led to a decrease in radiochemical yield (33 ± 4% vs 50 ± 4%). However, the specific activity of the final [^{11}C]R107474 solution was improved to 24–28 GBq/μmol at the end of synthesis (55 min after EOB) which is most probably caused by a higher concentration of formaldehyde in the hydrogen chloride solution in 1,4-dioxane compared to the hydrogen chloride solution in diethyl ether.

2.5. Biodistribution experiments in rats

Figure 4 summarizes the distribution of [^{11}C]R107474 in the blood, brain areas, and selected peripheral organs at 5, 10, 20, and 30 min after injection. The uptake of [^{11}C]R107474 is very rapid, in most tissues it reaches its maximum concentration at 5 min after tracer injection. Uptake in peripheral organs, except for the liver and kidney, is lower than in the examined brain areas. In the brain, the highest uptake was observed in septum (3.54 ± 0.52 ID/g, 5 min pi) and entorhinal cortex (1.57 ± 0.10 ID/g, 5 min pi) corresponding to the known high density of α_2-adrenoceptors in those regions.[26,27] To determine the target-to-non-target ratios in the brain, the amount of radioactivity in selected brain regions was compared to that in the cerebellum, an area with relatively low density of α_2-adrenoceptors. As a result of rapid uptake in the septum and entorhinal cortex and slow clearance from these tissues compared to those in the cerebellum, the target-to-non-target ratios increased with time (Fig. 5) which is a strong indication of selective binding to α_2-adrenoceptors. A tissue/cerebellum ratio of approximately 1 with no apparent maximum is considered indicative of non-specific binding. At 30 min after injection, tissue/cerebellum ratios of 5.38 ± 0.45 and 3.43 ± 0.24 were observed for the septum and entorhinal cortex, respectively. In comparison, a much lower uptake was displayed in the remainder of the dissected brain areas and cerebellum throughout the time course of the experiment (tissue/cerebellum ratios of 1.19–1.58, Fig. 5). R107474 has nanomolar affinity for 5-HT$_7$ receptors, and although the K_i (5 nM) is

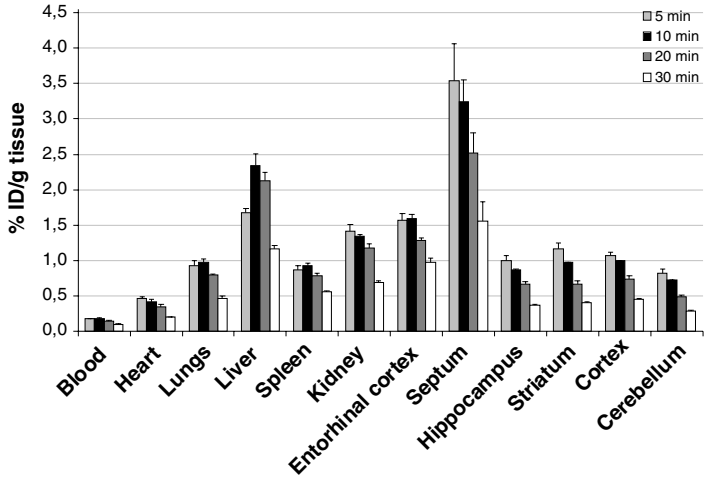

Figure 4. Tissue distribution of radioactivity after intravenous injection of [^{11}C]R107474 in rats. Data are means ± SEM (n = 4).

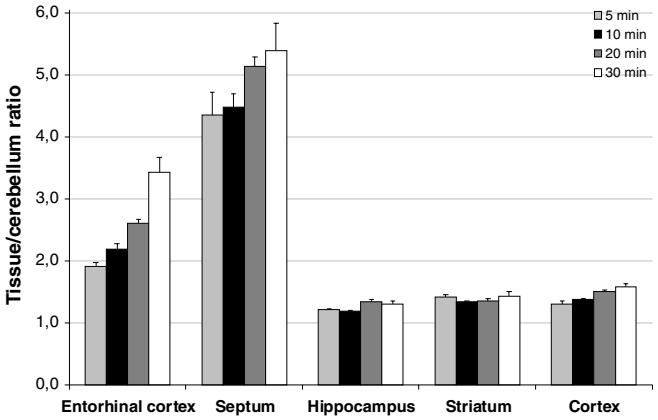

Figure 5. Tissue to cerebellum ratio of [^{11}C]R107474 in rat brain. Data are means ± SEM (n = 4).

40× higher than the K_i for α_{2A}-adrenoceptors, it could be asked whether 5-HT$_7$ receptors are also labeled by [^{11}C]R107474. As reviewed by Vanhoenacker et al.[28] the highest density of 5-HT$_7$ receptors is found in certain thalamic nuclei and a lower density occurs in the entorhinal cortex and some septal nuclei. The macroscopic dissection technique, applied in this study, is not suitable for dissection of thalamic nuclei and, therefore, potential labeling of the 5-HT$_7$ receptor could not be assessed.

To evaluate the possibility of specific inhibition of brain regional labeling using [^{11}C]R107474, a blocking experiment with mirtazapine was performed. In these experiments radiotracer accumulation in selected organs and brain regions was measured at 30 min post radiotracer injection and compared to that of saline-treated controls (Fig. 6). Pretreatment with mirtazapine (20 mg/kg, sc) 30 min before tracer injection significantly decreased uptake of [^{11}C]R107474 in all selected brain areas as compared to controls (Fig. 6). This result indicates that a large component of uptake of [^{11}C]R107474 in the septum and entorhinal cortex may be due to binding to α_2-adrenoceptors, although some labeling of 5-HT$_7$ receptors and inhibition of this labeling by mirtazapine cannot be excluded and needs further investigation.

3. Conclusion

The binding profile of R107474, being highly potent on α_2-adrenoceptor subtypes and on h5-HT$_7$ receptors and showing moderate to low binding affinities to the other receptors, as well as the in vivo α_{2A}- and α_{2C}-adrenoceptor occupancy, makes this compound of particular interest as a candidate for the development of a PET ligand to examine α_2-adrenoceptors in the brain.

[^{11}C]R107474 was synthesized in high radiochemical yield, purity, and specific activity. The in vivo biodistribution studies demonstrated that [^{11}C]R107474 shows high, fast, and specific uptake in α_2-adrenoceptor-rich brain areas. Based on these results, [^{11}C]R107474 will be further investigated as a potential radioligand for studying α_2-adrenoceptors using PET.

4. Materials and methods

4.1. In vitro receptor binding profile of R107474

The binding affinities in vitro (pIC_{50} values in $-\log M$ and K_i values in nanomolars) of R107474 for the various receptors, ion channel, and monoamine transporter

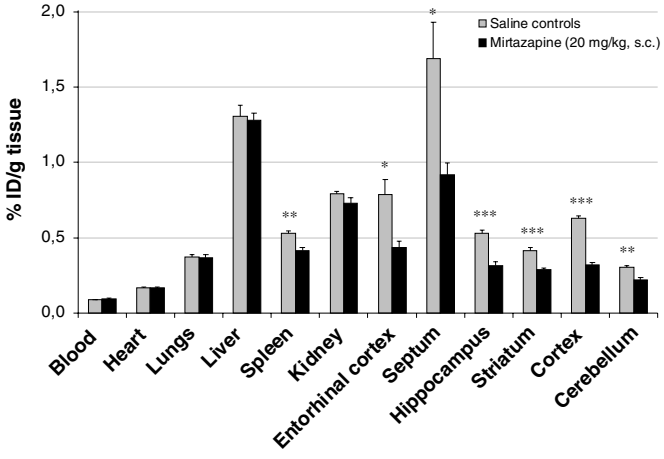

Figure 6. Effect of the non-selective α_2-adrenoceptor antagonist mirtazapine on the accumulation of [^{11}C]R107474 in selected organs and brain regions 30 min after injection of the radiotracer. Mirtazapine was administered 30 min prior to the radioligand (see Section 4). Data are means ± SEM (n = 4). Significant difference in percentage of ID/g tissue is marked with asterisks; $^*P < 0.05$, $^{**}P < 0.01$, and $^{***}P < 0.001$.

binding sites (see Table 2) were determined according to published methods.[20]

4.2. Ex vivo α_2-adrenoceptor occupancy of R107474

4.2.1. Drug treatment. Male Wistar rats weighing 180–220 g were housed in a rat raising facility on a 12 h light/dark cycle with food and water ad libitum. All procedures were conducted in strict accordance with the European Communities Council Directive of 24 November 1986 (86/609/EEC) and were approved by the Animal Care and Use Committee of Johnson and Johnson Pharmaceutical Research and Development.

Rats were treated by sc administration of vehicle or R107474 in the back at four dosages from 0.01 to 0.63 mg/kg body weight (three animals per dose). The animals were decapitated 1 h after drug administration. Brains were immediately removed from the skull and rapidly frozen in dry-ice cooled 2-methylbutane (−40 °C). Twenty micrometer thick sections were cut using a Leica CM 3050 cryostat-microtome (van Hopplynus, Belgium) and thaw-mounted on microscope slides (SuperFrost Plus, LaboNord, France). The sections were then kept at −20 °C until use.

4.2.2. Ex vivo radioligand binding in brain sections[22]. Selective occupancy measurement of α_{2A}-adrenoceptors was achieved by quantifying the specific binding of the subtype non-selective radioligand [^{3}H]RS79948-197 in the septum, a brain area expressing selectively the α_{2A}-adrenoceptor. To measure the occupancy of α_{2C}-adrenoceptors, we have used the property of [^{3}H]rauwolscine to label selectively this subtype in the rodent brain. α_{2C}-Adrenoceptor occupancy was quantified in the striatum, the brain area showing the highest α_{2C}-adrenoceptor density.

The following general procedure was applied. After thawing, sections were dried under a stream of cold air. The sections were not washed prior to incubation, in order to avoid dissociation of the drug-receptor complex. Brain sections of drug-treated and vehicle-treated animals were incubated in parallel for 10 min with the radioligands (3 nM [^{3}H]RS79948-197 in 50 mM Tris–HCl buffer, pH 7.4, for α_{2A}-adrenoceptor occupancy; 0.8 nM [^{3}H]rauwolscine in 50 mM Na/K phosphate buffer, pH 7.7, for α_{2C}-adrenoceptor occupancy). Non-specific binding was measured in adjacent sections (10 μM rauwolscine for [^{3}H]RS79948-197; 10 μM phentolamine for [^{3}H]rauwolscine). After the incubation, the excess of radioactivity was washed off in consecutive baths of ice-cold buffer (2× 1 min for [^{3}H]RS79948-197; 3× 10 min for [^{3}H]rauwolscine) followed by a quick rinse in ice-cold water. The sections were then dried under a stream of cold air.

4.2.3. Quantitative analysis. Quantitative autoradiography analysis was performed after 1 h acquisition with the β-imager (Biospace, Paris) according to our standard protocol.[29] Since only unoccupied receptors remain available for the radioligand, ex vivo receptor labeling is inversely proportional to the receptor occupancy by the in vivo administered drug. Percentages of receptor occupancy by the drug administered to the animal correspond to 100% − the percentage of receptor labeling in the treated animal. The percentage of receptor occupancy was plotted against dosage and the sigmoidal log dose–effect curve of best fit was calculated by non-linear regression analysis, using the GraphPad Prism program (San Diego, CA). From these dose–response curves, the ED_{50} (the drug dose producing 50% receptor occupancy) was calculated, with their 95% confidence limits.

4.3. Chemistry

The precursor for radiolabeling (**1**) and R107474[16] were synthesized at Johnson and Johnson Pharmaceutical Research and Development (Beerse, Belgium). Lithium aluminum hydride (LAH, 1.0 M in THF), hydrogen chloride (4.0 M in 1,4-dioxane and 2.0 M in diethyl ether), and formic acid were obtained from Sigma-Aldrich. LAH (0.1 M in THF) was acquired from ABX. Diisopropylamine (DIPA) was purchased from Merck-Schuchardt. Tetrahydrofuran (THF) was freshly distilled from LAH before use. All other chemicals and solvents were used as received unless otherwise stated. Reactions were performed under anhydrous conditions under a He-atmosphere. [^{11}C]Carbon dioxide was produced by the $^{14}N(p,\alpha)^{11}C$ nuclear reaction using an IBA Cyclone 18/9. Semi-preparative high performance liquid chromatography (HPLC) was performed with a Jasco PU-1587 preparative 50 mL/min pump (Maarssen, The Netherlands), an in-line Jasco PU-1575 ultraviolet (UV) detector (wavelength 265 nm), and a homemade flow-through radioactivity detector. Jasco-Borwin 1.5 HSS 1500 software was applied for data acquisition and processing. Radioactivity was quantified with a VDC-405 dose calibrator (Veenstra Instruments, Joure, The Netherlands). HPLC for analysis and quality control was performed with a LKB/Pharmacia 2249 pump, an in-line LKB/Pharmacia VWM 2141 UV detector (wavelength 265 nm), a flow-through NaI(Tl) crystal scintillation detection system, and Gina-Star version 2.12 (Raytest) for data acquisition and processing. All reactions were carried out in homemade, remotely controlled devices.[30]

4.3.1. Radiosynthesis of [^{11}C]formaldehyde. [^{11}C]CO_2, carried by a stream of helium with a flow of 10 mL/min, was bubbled into a mixture of LAH in THF (50 μL, 1 M) and dry THF (250 μL) at low temperature (see Table 2). After 2.5 min, the reaction was quenched with aqueous H_2SO_4 (300 μL, 2 M), HCl in 1,4-dioxane (150 μL, 4.0 M) or HCl in diethyl ether (300 μL, 2 M). Subsequently, the reaction vessel was heated to 120 °C for 4 min. The volatile content of the vessel was transferred via a stream of helium into a second vessel containing water. An aliquot was analyzed by HPLC using a mobile phase of 0.5 mM H_2SO_4 (pH 3.5) at a flow rate of 1.0 mL/min (Aminex HPX-87P, 300 × 7.8 mm; refractive index detector). Radioactive peaks corresponding to [^{11}C]CO_2, [^{11}C]CH_3OH and [^{11}C]formaldehyde were observed (t_R = 3.83 min, t_R = 5.68 min, and t_R = 4.23 min, respectively). The

optimum, decay-corrected [^{11}C]formaldehyde yield was 61 ± 7% as shown in Table 2.

4.3.2. Radiosynthesis of [^{11}C]R107474. [^{11}C]CO_2, carried by a stream of helium with a flow of 10 mL/min, was bubbled into a mixture of LAH in THF (300 μL, 0.1 M) at low temperatures (see Table 3). After 2.5 min, the reaction was quenched with HCl in 1,4-dioxane (90 μL, 4.0 M) or HCl in diethyl ether (180 μL, 2 M). Subsequently, the reaction vessel was heated to 120 °C for 4 min. The volatile content of the vessel was transferred via a stream of helium into a second vessel containing a solution of precursor **1** (1.0 mg) in water (50 μL) and formic acid (200 μL). The resulting mixture was then heated to predetermined temperatures (see Table 3) for 10 min to furnish [^{11}C]R107474. After evaporation of the solvents at 140 °C, the residue was diluted with DIPA (40 μL) in methanol (1.5 mL) and purified by semi-preparative HPLC (column: Kromasil C18, 10 μm, 250 × 21 mm; flow: 10 mL/min; eluent: MeOH/H_2O/DIPA, 90/10/0.2, v/v/v, $\lambda = 265$ nm). The fraction containing [^{11}C]R107474 ($t_R = 9.5$ min) was collected, diluted with water (50 mL), and the desired product was isolated by solid phase extraction using a Sep-Pak C18 plus. After washing with water (20 mL), the C18 cartridge was eluted with ethanol (0.5 mL) and the elute was diluted with saline.

Under the optimal reaction conditions (in terms of specific activity), the decay-corrected radiochemical [^{11}C]R107474 yield was 33 ± 4% ($n = 4$) and chemical and radiochemical purities were ⩾99% as determined by analytical HPLC. Specific activity was 24–28 GBq/μmol ($n = 4$) at the end of synthesis. The overall synthesis time, from EOB to formulated product, was 55 min.

4.4. Biodistribution and evaluation of inhibition of binding in vivo in rats

[^{11}C]R107474 (24–28 GBq/μmol) was injected into the tail vein of diethyl ether anesthetized male Wistar rats (200–250 g). The rats received 30–40 MBq (injected at the start of the experiment) in 300 μL saline including 10% (v/v) ethanol. The rats were sacrificed by cervical dislocation at 5, 10, 20, and 30 min post injection under diethyl ether anesthesia. A blood sample was taken by cardiac puncture and selected tissues were rapidly dissected and weighed. The radioactivity was measured using a LKB Wallac 1282 compugamma CS and the results expressed as percentage of injected dose per gram of tissue (% ID/g). For the blocking study, rats were administered either saline (200 μL, sc) or the non-selective α_2-adrenoceptor antagonist mirtazapine (20 mg/kg, sc) 30 min prior to radiotracer administration and the rats were sacrificed at 30 min post tracer injection. The significance between groups was evaluated using an unpaired two-tailed *t*-test. The criterion for significance was $P < 0.05$. All animal studies were performed with the approval of the Animal Experiment Ethical Committee of the Vrije Universiteit.

Acknowledgments

I. Lenaerts from Johnson and Johnson Pharmaceutical Research and Development is gratefully acknowledged for her assistance in the biodistribution experiments. P. J. van Leuffen and co-workers of the BV Cyclotron VU are acknowledged for the $^{11}CO_2$ production.

References and notes

1. Elhwuegi, A. S. *Prog. Neuropsychopharmacol. Biol. Psychiatry* **2004**, *28*, 435.
2. Millan, M. J. *Eur. J. Pharmacol.* **2004**, *500*, 371.
3. Payne, J. L.; Quiroz, J. A.; Zarate, C. A.; Manji, H. K. *Biol. Psychiatry* **2002**, *52*, 921.
4. Millan, M. J.; Lejeune, F.; Gobert, A. *J. Psychopharmacol.* **2000**, *14*, 114.
5. Ordway, G. A.; Schenk, J.; Stockmeier, C. A.; May, W.; Klimek, V. *Soc. Biol. Psychiatry* **2003**, *53*, 315.
6. Flugge, G.; van Kampen, N.; Meyer, H.; Fuchs, E. *Eur. J. Neurosci.* **2003**, *17*, 917.
7. Shiue, C.; Pleus, R. C.; Shiue, G. G.; Rysavy, J. A.; Sunderland, J. J.; Cornish, K. G.; Young, S. D.; Bylund, D. B. *Nucl. Med. Biol.* **1998**, *25*, 127.
8. Pleus, R. C.; Shiue, C.-Y.; Shiue, G. G.; Rysavy, J. A.; Huang, H.; Cornish, K. G.; Sunderland, J. J.; Bylund, D. B. *Receptor* **1992**, *2*, 241.
9. Solin, O.; Enas, J. D.; Bergman, J.; Haaparanta, M.; VanBrocklin, H. F.; Budinger, T. F. *J. Nucl. Med.* **1996**, *37*, S196.
10. Marthi, K.; Bender, D.; Watanabe, H.; Smith, D. F. *Nucl. Med. Biol.* **2002**, *29*, 317.
11. Hume, S. P.; Lammertsma, A. A.; Opacka-Juffry, J.; Ahier, R. G.; Myers, R.; Cremer, J. E.; Hudson, A. L.; Nutt, D. J.; Pike, V. W. *Nucl. Med. Biol.* **1992**, *19*, 841.
12. Hume, S. P.; Hirani, E.; Opacka-Juffry, J.; Osman, S.; Myers, R.; Gunn, R. N.; McCarron, J. A.; Clark, R. D.; Melichar, J.; Nutt, D. J.; Pike, V. W. *Eur. J. Nucl. Med.* **2000**, *27*, 475.
13. Robinson, E. S. J.; Tyacke, R. J.; Finch, L.; Willmott, G.; Husbands, S.; Nutt, D. J.; Hudson, A. L. *Neuropharmacology* **2004**, *46*, 847.
14. Enas, J. D.; Clark, R. D.; VanBrocklin, H. F.; Biegon, A.; Hanrahan, S. M.; Budinger, T. F. *J. Nucl. Med.* **1996**, *37*, S152.
15. Marthi, K.; Bender, D.; Gjedde, A.; Smith, D. F. *Eur. Neuropsychopharmacol.* **2002**, *12*, 427.
16. Kennis, L. E. J.; Bischoff, F. P.; Mertens, C. J.; Love, C. J.; Van den Keybus, F. A. F.; Pieters, S.; Braeken, M.; Megens, A. A. H. P.; Leysen, J. E. *Bioorg. Med. Chem. Lett.* **2000**, *10*, 71.
17. De Boer, T.; Ruigt, G. S. F.; Berendsen, H. H. G. *Hum. Psychopharmacol.* **1995**, *10*, S107–S118.
18. Kasper, S. *Int. Clin. Psychopharmacol.* **1995**, *10*, 25.
19. Van der Mey, M.; Leysen, J. E.; Windhorst, A. D.; Herscheid, J. D. M. *J. Labelled Compd. Radiopharm.* **2001**, *44*, S427–S429.
20. Leysen, J. E.; Gommeren, W.; Heylen, L.; Luyten, W. H. M. L.; Van de Weyer, I.; Vanhoenacker, P.; Haegeman, G.; Schotte, A.; Van Gompel, P.; Wouters, R.; Lesage, A. S. *Mol. Pharmacol.* **1996**, *50*, 1567.
21. Frazer, A. *J. Clin. Psychopharmacol.* **1997**, *17*, 25.
22. Marcus, M. M.; Jardemark, K. E.; Wadenberg, M.-L.; Langlois, X.; Hertel, P.; Svensson, T. H. *Int. J. Neuropsychopharmacol.* **2005**, *8*, 1.
23. Whaley, W. M.; Govindachari, T. R. *Org. React.* **1951**, *6*, 151.

24. Nader, M. W.; Zeisler, S. K.; Theobald, A.; Oberdorfer, F. *Appl. Radiat. Isot.* **1998**, *49*, 1599.
25. Roeda, D.; Crouzel, C. *Appl. Radiat. Isot.* **2001**, *54*, 935.
26. Scheinin, M.; Lomasney, J. W.; Hayden-Hixson, D. M.; Schambra, U. B.; Caron, M. G.; Lefkowitz, R. J.; Fremeau, R. T., Jr. *Mol. Brain Res.* **1994**, *21*, 133.
27. King, P. R.; Gundlach, A. L.; Louis, W. J. *Brain Res.* **1995**, *675*, 264.
28. Vanhoenacker, P.; Haegeman, G.; Leysen, J. E. *Trends Pharmacol. Sci.* **2000**, *21*, 70.
29. Langlois, X.; te Riele, P.; Wintmolders, C.; Leysen, J. E.; Jurzak, M. *J. Pharmacol. Exp. Ther.* **2001**, *299*, 712.
30. Windhorst, A. D.; ter Linden, T.; De Nooij, A.; Keus, J. F.; Buijs, F. L.; Schollema, P. E.; Van Rooij, L. F.; Herscheid, J. D. M. *J. Labelled Compd. Radiopharm.* **2001**, *44*, S1052–S1054.